



Inert failure strains of sodium aluminosilicate glass fibers

Nathan P. Lower^a, Richard K. Brow^{a,*}, Charles R. Kurkjian^b

^a Department of Ceramic Engineering, University of Missouri-Rolla, 222 McNutt Hall, Rolla, MO 65401, USA

^b Department of Ceramics and Materials Engineering, Rutgers University, Piscataway, NJ 08854, USA

Abstract

The inert failure strains (ϵ_f) of glass fibers from the compositional series $25\text{Na}_2\text{O} \cdot x\text{Al}_2\text{O}_3 \cdot (75 - x)\text{SiO}_2$, where $0 \leq x \leq 32.5$, were measured at 77 K using a two-point bending technique. Failure strain decreases when Al_2O_3 replaces SiO_2 , from 20.9% for $x = 0$ to 13.7% for $x = 32.5$. The failure strain depends on the testing speed, or faceplate velocity (V_{fp}) of the two-point bender. For glasses with relatively low alumina contents ($x < 10$), ϵ_f decreases with increasing V_{fp} , a behavior noted in an earlier study of sodium silicate glasses [J. Non-Cryst. Solids, in press]. For glasses with greater alumina contents ($x \geq 15$), ϵ_f shows little dependence on V_{fp} , as is found for silica fibers. The replacement of SiO_2 with Al_2O_3 strengthens the glass network through the replacement of non-bridging oxygens with oxygens that bridge neighboring alumina and silica tetrahedra. This stronger (more cross-linked) network is less distorted at high stresses and so does not allow such large strains before failure. The dependence of ϵ_f on testing rate (V_{fp}) appears to be related to the presence of non-bridging oxygens in the glass network and the relaxation of these sites, as indicated by internal friction studies of similar glasses. This may explain the greater values of ϵ_f at the slower V_{fp} for the less cross-linked networks.

© 2004 Elsevier B.V. All rights reserved.

PACS: 61.43.Fs; 62.20.Mk; 81.05.Kf; 81.70.Bt

1. Introduction

The two-point bend test is convenient for studying the effects of composition, processing conditions, and testing environment on the failure conditions for glass fibers [2]. The test measures the strain at failure by compressing a U-shaped fiber section between two plates, putting the outer portion of the U-bend in tension and the inner part in compression. The test is quick and fibers can be easily tested under liquid nitrogen to avoid environmental fatigue effects and so provide 'inert' failure information. Because strain is measured, the elastic modulus at failure must be known in order to calculate

failure strengths. While few details are available at high strains, it is known that the elastic modulus of silica initially increases with increasing strain [3], whereas the elastic modulus of multi-component glasses decreases with increasing strain [4]. Using zero-strain moduli (obtained by acoustic pulse techniques) with two-point bending strain data will overestimate the failure strengths of multi-component glasses, compared with conventional fiber tensile tests. Nevertheless, the failure strains obtained for pristine fibers by the two-point bend technique are sensitive to systematic changes in glass composition and structure. For example, we have shown [5] that the failure strains of $30\text{RO} \cdot 10\text{Al}_2\text{O}_3 \cdot 60\text{P}_2\text{O}_5$ glass fibers (where R = Na, K, Zn, Mg, Ca and Ba) increase as the field strength of the modifier increases, a trend that confirms earlier three-point bend studies of the strengths of alkali aluminophosphate glasses [6]. More recently we have found systematic increases in the failure strains in liquid nitrogen of a series of

* Corresponding author. Tel.: +1 573 341 6812; fax: +1 573 341 6934.

E-mail address: brow@umr.edu (R.K. Brow).

$x\text{Na}_2\text{O} \cdot (1-x)\text{SiO}_2$ with increasing x [1]. In addition, we found that the failure strain in liquid nitrogen depends on the rate at which the test is done.

In this paper we characterize the inert (liquid nitrogen) failure strains of pristine glass fibers drawn from sodium aluminosilicate glass melts using the two-point bending test and compare these results to those obtained in the earlier study of soda silicate glasses. The failure strain and the sensitivity of the failure strain to the testing rate depend on composition and appear to be related to the number of non-bridging oxygens associated with the silicate and aluminosilicate glass networks.

2. Experimental procedures

$25\text{Na}_2\text{O} \cdot x\text{Al}_2\text{O}_3 \cdot (75-x)\text{SiO}_2$ glasses, where $0 \leq x \leq 35$, were prepared from mixtures of reagent grade Na_2CO_3 , Al_2O_3 , and silica, melted in air in platinum crucibles for the times and at the temperatures indicated in Table 1. These times and temperatures were necessary to produce bubble-free melts. Weight loss measurements made prior to stirring indicate no significant volatilization losses (<1% relative) during melting, so the ‘as batched’ compositions will be used when discussing the glass properties and structure.

Glass fibers were drawn from the melts onto a rotating cage that ensures that pristine fibers are available for testing. Melt viscosities are controlled by the furnace temperature and by a water-cooled coil to produce fibers approximately 100–200 μm in diameter. Individual fibers approximately 10 cm long were removed from the cage and tested. The diameters of the fractured ends of individual fibers were measured using a micrometer ($\pm 0.5 \mu\text{m}$). Fibers free from crystals could not be drawn from the $x = 35$ melt and so the failure characteristics of these glasses were not determined.

Failure strains were measured using a two-point fiber bending system designed at UMR and fabricated by TNL Tool and Technology, LLC (Parnell, IA). Fiber

samples were immersed in liquid nitrogen (77 K) and the bender faceplates were driven together at rates (V_{fp}) between 50 and 4000 $\mu\text{m}/\text{s}$ until the fiber snapped and the failure was detected by an acoustic sensor. The failure strain (ε_f) was calculated from the faceplate gap distance at failure (D) and the fiber diameter (d) from [2]:

$$\varepsilon_f = 1.198d/(D-d). \quad (1)$$

At least 20 fibers were tested for each composition at each test condition. Because of the nature of the two-point bend test, a constant face plate velocity (FPV) produces a non-linear straining rate. Equivalent straining rates at failure for FPV's of 4000 and 5 are $\sim 60\%$ and $\sim 0.07\%$ strain per second respectively. The results are presented using the Weibull formalism

$$\ln \ln(1/(1-P)) = m \ln \varepsilon_f, \quad (2)$$

where P is the failure probability and m is the Weibull modulus, a measure of the reciprocal of the breadth of the failure distribution.

Fibers were tested under liquid nitrogen at different faceplate velocities (V_{fp}) to characterize ‘inert fatigue’ behavior. V_{fp} was varied continuously through a series of tests for a single composition and the data were then analyzed for each respective test condition. Elastic moduli were determined using an ultrasonic acoustic pulse technique [7] (Panatherm 5010, Panametrics, Massachusetts) for 100–200 μm diameter fibers drawn from each glass melt. Both extensional and torsional wave reflection times were obtained using twenty microsecond duration 200 kHz pulses. The sample length was measured and the respective extensional and torsional wave velocities were determined. At least nine samples of each composition were tested and Young's modulus (E) was calculated:

$$E = V_E^2 \times \rho. \quad (3)$$

Here, V_E is the extensional wave velocity and ρ is the glass density. Densities were measured using the Archi-

Table 1

Melting conditions, density, Young's modulus, failure strain and calculated failure strengths for $25\text{Na}_2\text{O} \cdot x\text{Al}_2\text{O}_3 \cdot (1-x)\text{SiO}_2$ glasses (strengths calculated from the 4000 $\mu\text{m}/\text{s}$ strains and the ‘zero strain’ Young's modulus)

Composition (mol%)			Melting conditions		Density (g/cc)	Young's modulus (GPa)	ε_f (%) at 4000 $\mu\text{m}/\text{s}$	ε_f (%) at 50 $\mu\text{m}/\text{s}$	Strength (GPa)
Na_2O	Al_2O_3	SiO_2	Temp ($^\circ\text{C}$)	Time (h)					
25	0	75	1300	6:30	2.4299 ± 0.0007	56.18 ± 0.33	20.85 ± 0.12	21.99 ± 0.10	11.71
25	5	70	1300–1400	11:30	2.4504 ± 0.0015	60.28 ± 0.34	19.48 ± 0.08	19.90 ± 0.11	11.74
25	10	65	1300–1450	10:00	2.4663 ± 0.0014	63.64 ± 0.37	17.81 ± 0.09	17.94 ± 0.12	11.33
25	15	60	1500	15:00	2.4768 ± 0.0015	67.34 ± 0.33	15.87 ± 0.11	15.87 ± 0.10	10.69
25	20	55	1550	17:00	2.4853 ± 0.0008	69.47 ± 0.28	15.17 ± 0.08	15.18 ± 0.09	10.54
25	25	50	1600	19:00	2.4923 ± 0.0014	70.98 ± 0.33	14.74 ± 0.09	14.78 ± 0.11	10.46
25	30	45	1600	23:45	2.5152 ± 0.0010	74.91 ± 0.17	14.42 ± 0.11	14.22 ± 0.09	10.80
25	32.5	42.5	1600	12:00	2.5263 ± 0.0002	76.72 ± 0.15	13.71 ± 0.08	13.45 ± 0.06	10.52
25	35	40	1650	7:00	2.5386 ± 0.0009	78.51 ± 0.30	–	–	–

medes method with kerosene as the buoyancy fluid. Fiber failure strengths (σ_f) are calculated from the failure strains (ϵ_f) and the respective (zero strain) Young's moduli.

3. Results

The densities and Young's moduli for the sodium aluminosilicate glasses prepared for this study are given in Table 1. These properties are in good agreement with those reported in an earlier study of similar glasses [8].

Weibull plots of the failure strains of the $25\text{Na}_2\text{O} \cdot x\text{Al}_2\text{O}_3 \cdot (75-x)\text{SiO}_2$ glass fibers tested under liquid nitrogen at face plate velocities (V_{fp}) of $4000 \mu\text{m/s}$ are shown in Fig. 1. In general, tight failure distributions (Weibull moduli > 150 , indicating relative standard deviations under $\sim 0.8\%$) could be obtained. Two sets of fibers were drawn for several compositions ($x = 0, 5, 10, 25, 30, 32.5$) and excellent reproducibility of the failure strain distributions was achieved, as shown in Fig. 1. Failure strains decrease with increasing Al_2O_3 -content, from $20.85 \pm 0.12\%$ for $x = 0$ to $13.71 \pm 0.08\%$ for $x = 32.5$ (inset, Fig. 1).

Fig. 2 shows failure strain distributions for several fiber compositions tested under liquid nitrogen using faceplate velocities (V_{fp}) of 50 and $4000 \mu\text{m/s}$. The failure strain (ϵ_f) is generally greater at the lower V_{fp} , particularly for the low alumina glasses ($x < 10$). For glasses with greater alumina contents (up to $x \sim 25$), ϵ_f changes little with changing V_{fp} (Fig. 3). The failure strain of the $x = 30$ and 32.5 fibers is lower at the slower breaking speeds, a behavior similar to that reported for fused silica fibers [1].

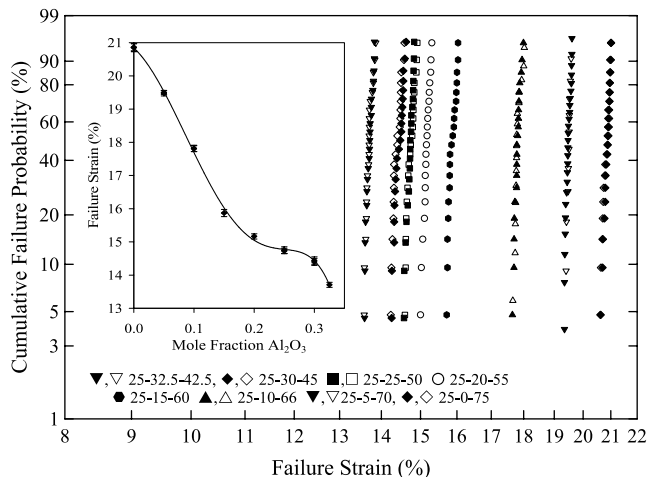


Fig. 1. Weibull distributions of the failure strains at liquid nitrogen for $25\text{Na}_2\text{O} \cdot x\text{Al}_2\text{O}_3 \cdot (75-x)\text{SiO}_2$ glass fibers (strain rate is 4000s). The respective average failure strains (ϵ_f) and Weibull moduli (m) are listed in Table 1. The inset shows the effects of x on ϵ_f .

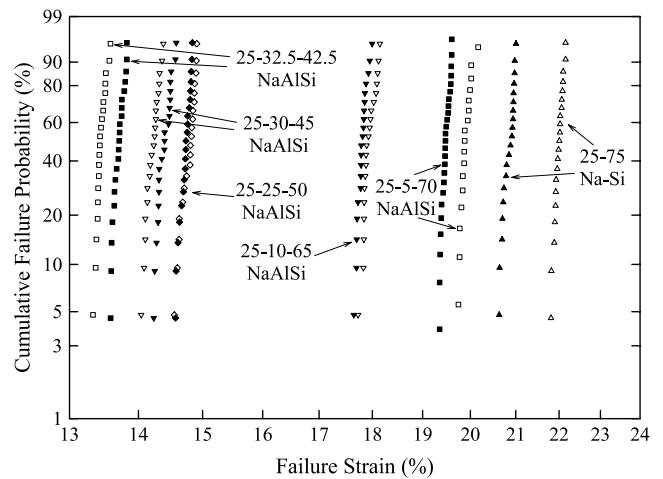


Fig. 2. Weibull distributions of the failure strains at liquid nitrogen for $25\text{Na}_2\text{O} \cdot x\text{Al}_2\text{O}_3 \cdot (75-x)\text{SiO}_2$ glass fibers measured with face plate velocities of $50 \mu\text{m/s}$ (open figures) and $4000 \mu\text{m/s}$ (closed figures).

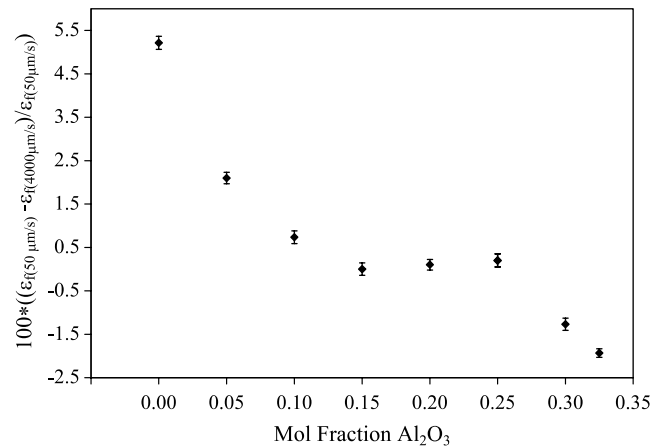


Fig. 3. Normalized difference in failure strains for $25\text{Na}_2\text{O} \cdot x\text{Al}_2\text{O}_3 \cdot (75-x)\text{SiO}_2$ glass fibers measured with face plate velocities of 50 and $4000 \mu\text{m/s}$.

4. Discussion

Fibers with the composition $25\text{Na}_2\text{O} \cdot 25\text{Al}_2\text{O}_3 \cdot 50\text{SiO}_2$ have an average failure strain of 14.7% ($V_{fp} = 4000 \mu\text{m/s}$) in liquid nitrogen. Based on the Young's modulus as determined by our acoustic pulse technique (71.0 GPa), we calculate a failure 'strength' of 10.4 GPa . This compares to a value of 8.5 GPa reported for the failure strength in a three-point bend test under liquid nitrogen of fibers with the same nominal composition [9]. The present study almost certainly overestimates the true failure strength because we do not account for the anticipated reduction in elastic modulus with increasing levels of strain. (For example, using our measured failure strain of 14.7% with the reported failure strength of 8.5 GPa , one calculates an elastic modulus at failure of $\sim 60 \text{ GPa}$, compared with our measured zero strain modulus of 71.0 GPa .)

The inert failure strain (ϵ_f) of $25\text{Na}_2\text{O} \cdot x\text{Al}_2\text{O}_3 \cdot (75 - x)\text{SiO}_2$ glass fibers decreases with increasing x (Fig. 1). Replacing silica with alumina reduces the number of non-bridging oxygens in the network structure and the greater bonding energy of the bridging oxygens between neighboring silicate and aluminate tetrahedra yields a stiffer structure [10], as indicated by the increase in Young's modulus (Table 1). The presence of non-bridging oxygens appears to allow the glass network to deform more prior to failure. Fig. 4 plots the liquid nitrogen failure strains of the sodium aluminosilicate fibers and of binary sodium silicate fibers, obtained in an earlier study [1], against the number of non-bridging oxygens per glass former (Si + Al), calculated from each respective glass composition. The non-bridging oxygens in both series accommodate the network distortions associated with the very large stresses that are imparted to the fibers prior to failure. We assume that no non-bridging oxygens are present in the 'alumina-rich' ($x = 30$) glass and that the excess alumina is associated with oxygen-triclusters [11].

The distortion (or relaxation) of non-bridging oxygens in the glass structure may also be responsible for the dependence of ϵ_f on the faceplate velocity (V_{fp}) used during the test (Fig. 2). Fig. 5 compares the normalized change in ϵ_f for tests at 50 and 4000 $\mu\text{m/s}$ for the sodium aluminosilicate glass fibers and for the sodium silicate glass fibers, analyzed in an earlier study, with their respective concentrations of non-bridging oxygens. In both series, a greater change in ϵ_f with V_{fp} is associated with glasses that possess greater concentrations of non-bridging oxygens. It is important to note that the V_{fp} effect does not appear to be dependent on the Na_2O -concentration or simply on the expected mobilities of the Na^+ ions. (Na^+ mobility in the $\text{Na}-25\text{Na}_2\text{O} \cdot x\text{Al}_2\text{O}_3 \cdot (75 - x)\text{SiO}_2$ series will be greatest when $x = 25$ [12] and changes in alkali transport behavior

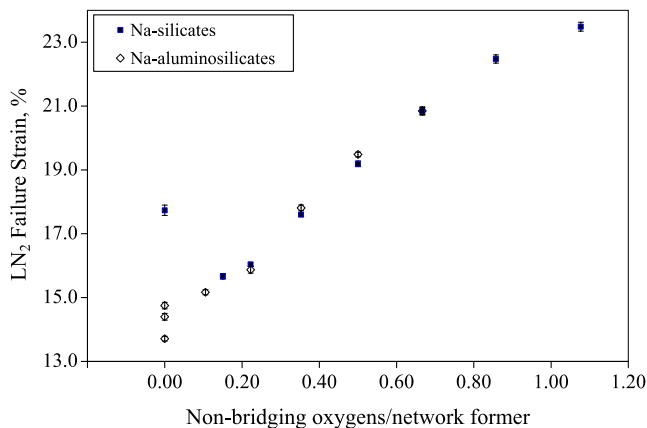


Fig. 4. The effect of non-bridging oxygens on the failure strains of $x\text{Na}_2\text{O} \cdot (100 - x)\text{SiO}_2$ [1]. $25\text{Na}_2\text{O} \cdot x\text{Al}_2\text{O}_3 \cdot (75 - x)\text{SiO}_2$ glass fibers. Note that we assume the $x = 30$ and glasses possess no non-bridging oxygens.

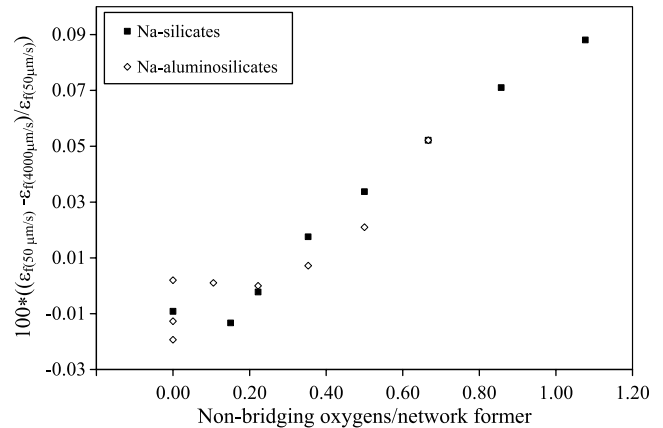


Fig. 5. The effect of non-bridging oxygens on the inert delayed failure effect for $x\text{Na}_2\text{O} \cdot (100 - x)\text{SiO}_2$ [1] and $25\text{Na}_2\text{O} \cdot x\text{Al}_2\text{O}_3 \cdot (75 - x)\text{SiO}_2$ glass fibers. Note that we and 32.5 glasses possess no non-bridging oxygens.

have been proposed to explain the strengthening of mixed alkali glasses [13].) Thus, it appears that the increase in failure strain at slower faceplate velocities is not necessarily caused by a relaxation of the structure as alkali ions move from the high compression to the high tensile regions of the strained fibers. Instead, it appears that the glass network responds by distortions associated with the non-bridging oxygens. Removing non-bridging oxygens from the structure by adding alumina or by reducing the soda content makes the network stiffer and less responsive to the applied stress, as well as less sensitive to testing rates (V_{fp}). Relaxation of a silicate network through motions associated with the non-bridging oxygens has been used to explain features found in the internal friction spectra collected from Na-aluminosilicate glasses [14]. The relaxation of structural sites vacated by a diffusing ion through the re-configuration of non-bridging oxygens is an important aspect of recent studies of alkali transport phenomena [15].

5. Conclusions

The inert failure strains of sodium aluminosilicate glass fibers decrease with increasing alumina concentrations. This decrease reflects the stiffening of the silicate network with decreasing concentrations of non-bridging oxygens. The presence of non-bridging oxygens allows the glass network to more readily deform in response to the applied stress, leading to a larger strain before failure. The inert failure strains of $25\text{Na}_2\text{O} \cdot x\text{Al}_2\text{O}_3 \cdot (75 - x)\text{SiO}_2$ glasses increase with lower applied stressing rates (V_{fp}) when $x < 10$, and is insensitive to V_{fp} when $x \geq 15$. This inert delayed failure effect was also noted in an earlier study of alkali silicate fibers [1] and may be a consequence of the relaxation of

non-bridging oxygens in the glass structure with the applied stress.

Acknowledgement

The authors thank the NSF/Industry/University Center for Glass Research for support in the development of the fiber preparation and testing equipment at UMR.

References

- [1] N.P. Lower, R.K. Brow, C.R. Kurkjian, *J. Non-Cryst. Solids*, in press.
- [2] M.J. Matthewson, C.R. Kurkjian, S.T. Gulati, *J. Am. Ceram. Soc.* 69 (1986) 815.
- [3] J.T. Krause, L.R. Testardi, R.N. Thurston, *Phys. Chem. Glasses* 20 (6) (1979) 135.
- [4] R. Bruckner, G. Pahler, C.R. Kurkjian (Ed.), *Strength of Inorganic Glass*, Plenum Press, New York, p. 329.
- [5] R.K. Brow, N.P. Lower, A.J. Lang, C.R. Kurkjian, *Glastech. Ber.* 75 (C2) (2002) 133.
- [6] L.G. Baikova, Yu.K. Fedorov, V.P. Pukh, et al., *Fiz. Khim. Stekla (Engl. Trans.)* 19 (1993) 380.
- [7] L.C. Lynnworth, *J. Testing, Evaluation* 1 (1973) 119.
- [8] V.Ya. Livshits, D.G. Tennison, S.B. Gukasyan, K.A. Kostanyan, *Fizika I Khimiya Stekla* 8 (6) (1982) 688.
- [9] T.I. Pesina, L.G. Baikova, V.P. Pukh, I.I. Novak, M.F. Kireenko, *Fiz Khim Stekla* 12 (1) (1986) 26.
- [10] A. Makishima, J.D. Mackenzie, *J. Non-Cryst. Solids* 12 (1973) 35.
- [11] A. Osaka, M. Ono, K. Takahashi, *J. Am. Ceram. Soc.* 70 (4) (1987) 242.
- [12] R. Terai, *Phys. Chem. Glasses* 10 (4) (1969) 146.
- [13] V.A. Bershtein, Yu.A. Emel'yanov, V.A. Stepanov, *Fiz. Khim. Stekla* 9 (1983) 74.
- [14] D.E. Day, G.E. Rindone, *J. Am. Ceram. Soc.* 45 (10) (1962) 489.
- [15] A. Bunde, K. Funke, M.D. Ingram, *Sol. State Ionics* 86–88 (1996) 1311.